ChemComm

An Axially Chiral 1,1′-Biazulene and Its π-Extended Derivative: Synthesis, Structures and Properties

Journal:	*ChemComm*
Manuscript ID	CC-COM-05-2019-003510.R2
Article Type:	Communication

ARTICLE

An Axially Chiral 1,1′-Biazulene and Its π-Extended Derivative: Synthesis, Structures and Properties

Received 00th January 20xx,
Accepted 00th January 20xx

DOI: 10.1039/x0xx00000x

Chaolumen, [ab] Hideto Ito *[ab] and Kenichiro Itami *[abc]

Chiral organic π-conjugated molecules have been intensively investigated in the fields of chiral electronic materials and devices. Herein we report a new motif for the axially chiral 1,1′-biazulene and its π-extended derivative, in which biphenyl was annulated by electron-rich five membered-ring of azulene moiety. These two compounds were unexpectedly synthesized from 2-terphenyl azulene by stepwise intermolecular and intramolecular oxidative C–H/C–H couplings. X-ray diffraction analysis revealed that the crystals of both compounds contain a pair of enantiomers. Furthermore, the axially chiral 1,1′-biazulene derivatives were successfully separated into enantiomers that exhibited clear mirror-image circular dichroism spectra up to near-infrared region.

Introduction

The demand for organic π-conjugated molecules with axial chirality becomes significantly important in association with the developments of chiral electronic materials and devices. For this reason, organic molecules, such as helicenes[1] and their axially chiral analogues[2] have been extensively investigated over the last several decades. Among various organic π-conjugated molecules, azulene, an structural isomer of naphthalene, has unusual structural, optical and electronic properties.[3] Azulene possesses a 10π non-benzenoid structure which consists of one electron-rich five-membered ring and one electron-deficient seven-membered ring with a dipole moment of 1.08D so as to receive aromatic stabilization.[4] Consequently, these electronic features distinguish azulene from other typical fused benzenoids by non-mirror-related HOMO/LUMO geometry. In addition, azulene exhibits a small HOMO–LUMO gap and a weak $S_0 \rightarrow S_1$ transition in the visible region, which makes azulene as one of the smallest conjugated systems having a visible chromophore with blue color.[5] These interesting electronic and photophysical properties make azulene a promising building block for construction of new optoelectronic materials. Currently, a number of azulene-based π-conjugated materials have been synthesized and developed as useful materials in various research fields.[3,6-15]

Among these azulene-based π-conjugated molecules, biaryl compounds, such as the 1,1′-biazulene, are considered to be isomers of 1,1′-binaphthyl compounds that have been widely used in asymmetric synthesis as axially chiral auxiliaries.[16] Considering azulene's unique structural and optoelectronic features, potential properties and applications of axially chiral 1,1′-biazulene derivatives would be promising and worthy for exploration. However, the intrinsic instability of 1-haloazulene limits efficient aryl-aryl coupling of azulene.[8f] Additionally, very few axially chiral 1,1′-biazulene derivatives[17,18] (Fig. 1a) have been reported because five- and seven-membered rings of azulene moiety exhibit less hindered rotation around aryl–aryl bond, compared to 1,1′-binaphthalene. Herein we report a 1,1′-biazulene **1** and its π-extended derivative **2**, which were unexpectedly synthesized from 2-terphenyl azulene by stepwise intermolecular and intramolecular C–H/C–H couplings (Fig. 1b). In addition, X-ray crystallographic structures, the isolation of stable axially chiral 1,1′-biazulenes, and photophysical and electrochemical properties derived from intriguing π-systems are also investigated.

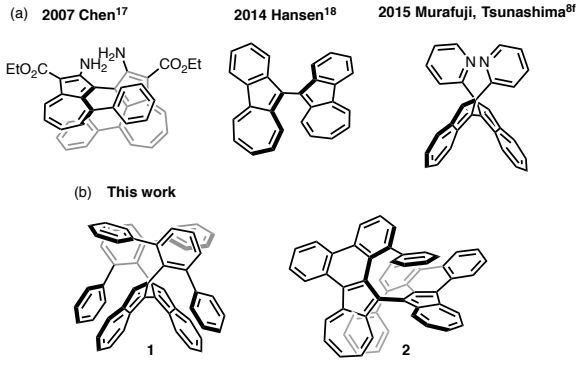

Fig. 1 (a) Chemical structures of representative axially chiral biazulene derivatives and (b) the molecules reported in this work.

[a] *JST-ERATO, Itami Molecular Nanocarbon Project, Nagoya University, Chikusa, Nagoya, 464-8602 (Japan)*
E-mail: Itami@chem.nagoya-u.ac.jp, ito.hideto@g.mbox.nagoya-u.ac.jp
[b] *Graduate School of Science, Nagoya University, Chikusa, Nagoya, 464-8602 (Japan)*
[c] *Institute of Transformative Bio-Molecules (WPI-ITBM), Nagoya University, Chikusa, Nagoya, 464-8602 (Japan)*

† Electronic Supplementary Information (ESI) available: Syntheses, NMR, UV-vis-nearIR absorption, CV, DFT calculations and crystallographic table. CCDC 1899599 (**1**), 1899597 (**2**) and 1899598 (**4**). For ESI and crystallographic data in CIF or other electronic format see DOI: 10.1039/x0xx00000x

Results and Discussions

Synthesis and Structures

The synthesis of 1,1′-biazulenes was conducted by using 2-terphenyl azulene **3** which was easily derived from azulen-2-yl-boronic acid pinacol ester and 2,6-dipheny-1-iodobenzene by Suzuki–Miyaura cross-coupling (Scheme 1). On the course of oxidative dehydrogenation of **3** according to the previous related reports,[19] treatment with $FeCl_3$ as an oxidant induced the intermolecular C–H/–C–H coupling of **3** to afford 1,1′-biazulene **1** in 88% yield as a deep blue solid. In contrast, cyclodehydrogenation product **4** was isolated only in 8% yield, which was initially designed as a potential molecule for organic filed-effect transistor application. Furthermore, under the same oxidative conditions, we observed that the isolated **1** underwent intramolecular cyclodehydrogenation to give a π-extended 1,1′-biazulene derivative **2** in 33% yield as a greenish-yellow solid. Oligomers of **3** were not observed in the mass and ^{1}H NMR spectra. Several attempts for the one-pot synthesis of **2** from **3** resulted in the formation of trace amount of **2**. The reason for this is likely that the intermediate **1** is immediately protonated by in situ-generated HCl under oxidative conditions, which inhibits further oxidation of **1** to undergo intramolecular cyclization.[20] Due to the electron-rich properties of the five-membered ring in azulene, oxidative reactions usually prefer to take place at the C1 and C3 positions on azulene of **3**. Actually, DFT calculations for the radical cation $\mathbf{3}^{\bullet+}$ indicate that large spin densities locate on C1 and C3 positions, which lead aryl–aryl coupling between azulene moieties (see Fig. S11 in SI for details).[19b,21] In the case of $\mathbf{1}^{\bullet+}$, the Mülliken spin density resides almost completely on the azulene core, and negligible spin density is delocalized over the phenyl groups, indicating that radical cation pathway is not suitable to explain the reaction mechanism of intramolecular cyclization (Fig. S11 and Table S8). In the measurements of cyclic voltammetry (CV), **1** exhibited two-stage oxidation waves with poor reproducibility (Fig. S9 and S10). These theoretical and experimental studies indicated that the intramolecular cyclization of **1** is likely to proceed by the dication pathway.[19b]

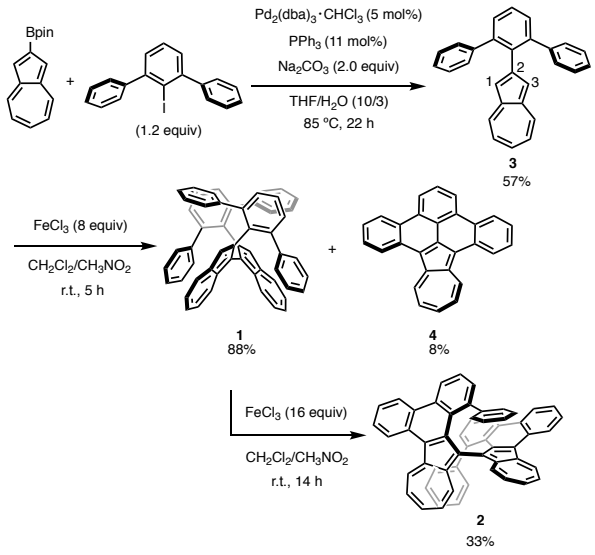

Scheme 1 Oxidative C–H/C–H coupling of 2-terphenyl-azulene **3** for synthesis of 1,1′-biazulenes **1** and **2**. Abbreviations: Bpin=4,4,5,5-tetramethyl-1,3,2- dioxaborolan-2-yl; dba=dibenzylideneacetone.

The ^{1}H NMR spectra of **1** and **2** indicated the existence of single conformers, respectively. Due to the bulky terphenyl groups and the sterically congested helical structure, we expected there are stable and isolable atropisomers of **1** and **2**. To our delight, the molecular structures of **1**, **2** and **4** were unambiguously determined by the single crystal X-ray diffraction analysis (Fig. 2 and S1–S6).[22] These results also reveal that the crystals of **1** and **2** contain a pair of enantiomers. The distance between the phenyl rings and azulene moieties for **1** and **2** is 3.15 Å and 3.34 Å, and these effective intramolecular π-π interactions lock the dihedral angles between the azulene moieties (64.7° for **1** and 64.9° for **2**) and restrict the free rotation of phenyl rings. Actually, in measurements of ^{1}H NMR spectra, we observed five non-equivalent proton signals derived from fixed phenyl rings of **2** (see SI for details). In the intramolecular C–H/C–H coupling reaction of **1**, the formation of *twisted*-**2** with two-fold symmetry was not observed at all**,** which was calculated to be unstable by ΔE = 23.2 kcal/mol compared with (*S*)-**2** or (*R*)-**2** probably because of the large strain energy that results from the highly bent structure of phenanthroazulene around the C–C bond between azulene moieties (Fig. S12). In addition, no transition state was observed in the transformation from (*S*)-**2** or (*R*)-**2** to *twisted*-**2** regardless of several calculations with different initial structures, methods and levels. It should be mentioned that each enantiomer of compound **1** and **2** is rather unstable in solution and easy to be decomposed in the heating condition at 40 °C. However, in the solid state, they do not show decomposition even when heated above the melting-point temperatures (Fig. S18 and S19).

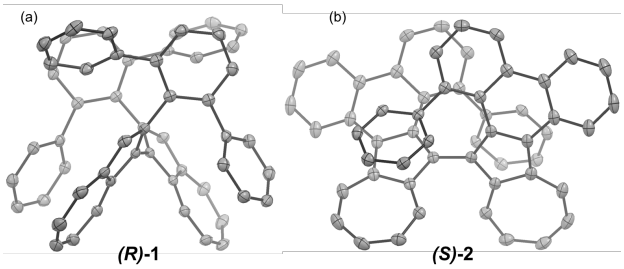

Fig. 2 ORTEP drawings of single-crystal structures of **1** and **2** with 50% probability.[22] (a) Molecular structure of (*R*)-**1**. (b) Molecular structure of (*S*)-**2**.

Electronic and Photophysical Properties

Next, cyclic voltammetry (CV) of **1**, **2, 3** and **4** were performed to clarify the electronic properties (Fig. S9 and S10). In the oxidation process, anodic peak potentials (E_{pa}) were recorded for comparison. Compound **3** shows one-stage oxidation wave (E_{pa} = +0.68 V vs. Fc/Fc^+) with poor reproducibility, while the dimer **1** exhibits two-stage oxidation waves (E_{pa} = +0.33 V and +0.85 V). Additionally, the second oxidation wave of **1** is irreversible with low reproducibility, indicating that, in the presence of strong oxidant like $FeCl_3$, unstable dication $\mathbf{1}^{2+}$ can be generated and likely to involve as the intermediate in the intramolecular cyclization of **1** to **2**. Compound **4** showed featureless but reproducible wave (E_{pa} = +0.28 V) in several circles, probably due to the effect of aggregation. Compound **2** shows three-stage waves (E_{pa} = +0.21 V, +0.64 V, and

+1.40 V), whereby the first oxidative wave is negatively shifted by ΔE_{pa} = 0.12 V and 0.47 V with respect to that of **1** and **3**, indicating its strong electron-donating ability due to the effective elongation of π-conjugation over two electron-rich five-membered rings on 1,1′-azulene. In the reduction process, compound **1**, **2**, and **3** showed irreversible waves between –2.16 V and –2.43 V, but the difference is apparently smaller than those observed in the oxidation process, indicating their similar LUMO energy levels. While compound **4** exhibit the reduction wave protentional at –1.88 V, indicating the lower LUMO level with respect to those of **1**, **2** and **3**. These results are also supported by DFT calculations (Fig. S13).

The absorption spectra of **1** and **3** are quite similar, exhibiting main absorption around 310 nm with a shoulder from 330–440 nm and the longest absorption centered around 590 nm (Fig. 3). While compared to **1** and **3**, to due the effective π-extension, compound **4** showed red-shifted the main absorption at 372 nm and the longest absorption at 695 nm. Additionally, reflecting the π-extended structure and high-lying HOMO, **2** exhibited the main absorption peak at 349 nm (log ε = 4.94) with a broad shoulder peaks around 400–500 nm. The longest absorption centered at 683 nm (log ε = 2.61), tailing up to 900 nm, is remarkably red-shifted compared to those of **3** and **1** by 98 and 90 nm, respectively. All these results are well supported by TD-DFT calculations (Fig. S13). In stark contrast to 1,1′-binaphthyl compounds, the 1,1′-biazulene derivatives **1** and **2** are not emissive. It is well known that azulene exhibits weak emission, however, all the reported 1,1′-biazulene derivatives are not emissive probably because of their strong vibrations around the aryl-aryl bond.[8f,17,18,22]

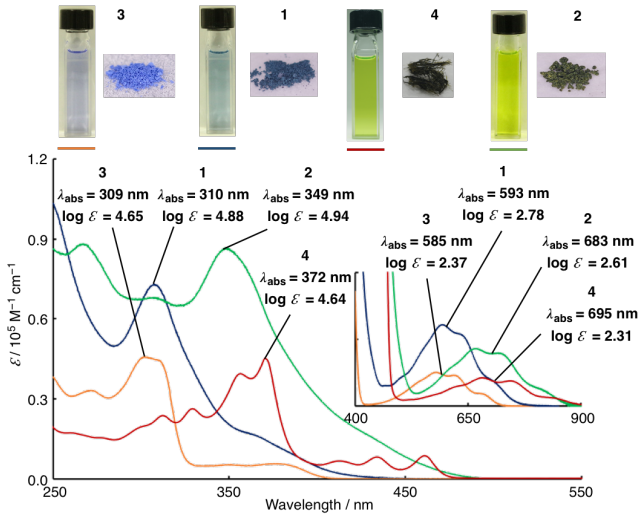

Fig. 3 The UV-Vis-NIR absorption spectra of **1**, **2**, **3** and **4** in CH_2Cl_2. The pictures of their CH_2Cl_2 solutions and powders are included.

Finally, the racemic mixtures of **1** and **2** were successfully separated by chiral HPLC (Fig. S7 and S8). The absolute configuration of the axial chirality of **1** and **2** was determined through comparison of the experimental CD spectra with those obtained in TD-DFT calculations (Fig. S14 and S15). The first eluted peaks for **1** and **2** in the chiral HPLC analyses were suggested to be (*R*)-**1** and (*R*)-**2**, respectively. For enantiomers of both **1** and **2**, the circular dichroism (CD) spectra (Fig. 4) exhibited the mirror-imaged spectra having strong Cotton effects at 256, 308 and 337 nm for **1** and 282, 333, 358 and 404 nm for **2** in the UV-Vis region, respectively, indicating that each fraction consists of enantiomers with opposite chirality. Due to the strong absorption coefficients, the intensity of the main bands for **1** and **2** (308 nm for **1**: $|\Delta\varepsilon|$ = 74.4 $M^{-1}\cdot cm^{-1}$, $|g_{CD}| = |\Delta\varepsilon/\varepsilon| = 1.0\times10^{-3}$; 404 nm for **2**: $|\Delta\varepsilon|$ = 33.1 $M^{-1}\cdot cm^{-1}$, $|g_{CD}| = 1.2\times10^{-3}$) are stronger than those of other helical-based signals (Tables S2 and S3), though the dissymmetry factor $|g_{CD}|$ is small. It is notable that the compounds **1** and **2** shows quite weak absorption coefficients and Cotton effects at longer wavelength regions, but detectable mirror image-like bands were also observed around 600–700 nm. From the calculations, those g_{CD} values (596 nm for (*R*)-**1**: $|\Delta\varepsilon|$ = 1.7 $M^{-1}\cdot cm^{-1}$, $|g_{CD}| = 2.8\times10^{-3}$; 626 nm for (*S*)-**1**: $|\Delta\varepsilon|$ = 0.4 $M^{-1}\cdot cm^{-1}$, $|g_{CD}| = 7.4\times10^{-4}$; 686 nm for (*R*)-**2**: $|\Delta\varepsilon|$ = 0.3 x $M^{-1}\cdot cm^{-1}$, $|g_{CD}| = 5.5\times10^{-4}$; 666 nm for (*R*)-**2**: $|\Delta\varepsilon|$ = 0.3 x $M^{-1}\cdot cm^{-1}$, $|g_{CD}| = 7.0\times10^{-4}$) were not low compared to those at shorter wavelength regions. These observations indicate that the contribution of the frontier orbitals of azulene moieties are effectively incorporated to the helical segments, and π-extensions at five-membered rings on chiral 1,1′-biazuene represents one of potential strategies for the creation of azulene-based chiroptical materials.

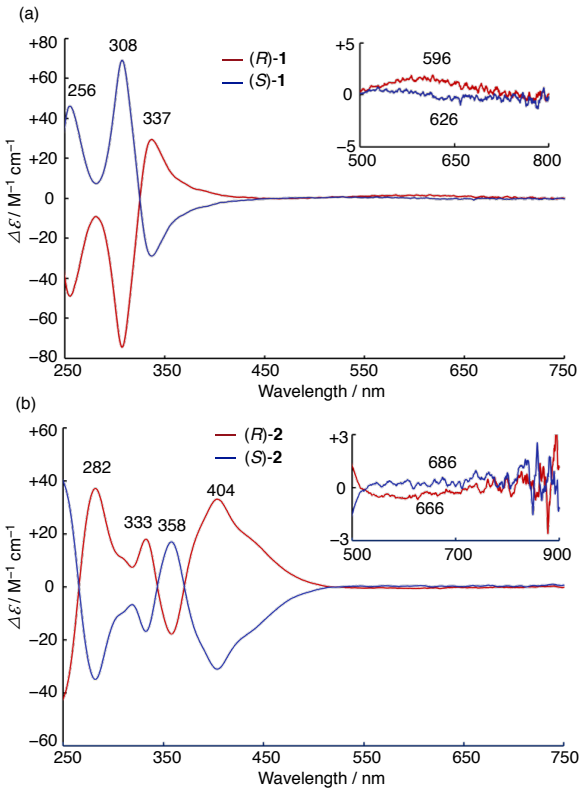

Fig. 4 (a) CD spectra of enantiopure (*R*)-**1** (red line, the first fraction) and (*S*)-**1** (blue line, the second fraction) eluted from *n*-hexane/CH_2Cl_2 (7:3) at 30 °C. (b) CD spectra of enantiopure (*R*)-**2** (red line, the first fraction) and (*S*)-**2** (blue line, the second fraction) eluted from *n*-hexane/CH_2Cl_2 (1:1) at 40 °C. All separations were conducted in HPLC equipped with a CHIRALPAK® ID column at the flow rate of 0.6 mL/min for **1** and 1.0 mL/min for **2**.

Conclusions

In summary, we have synthesized axially chiral 1,1′-biazulene **1** and its π-extended derivative **2**, which were synthesized by

stepwise intermolecular and intramolecular oxidative C–H/C–H couplings from 2-terphneyl azulene. The structures of **1** and **2** were unambiguously confirmed by single-crystal X-ray diffraction analysis, which also revealed that their crystals contain a pair of enantiomers. The enantiomers of **1** (*S* and *R*) and **2** (*S* and *R*) were successfully separated by chiral HPLC and exhibited clear mirror-image CD spectra up to 800 nm and 900 nm, respectively. Furthermore, CV measurements indicated that the π-extended derivative **2** exhibited a high-lying HOMO on account of the π-extended network by the electron-rich five-membered ring of the azulene moiety, which is reflected in the longest absorption centred at 683 nm, tailing up to 900 nm. The electronic and photophysical properties of **2** make it attractive for future application as optoelectronic materials. The efficient synthetic method reported here should be highly general and applicable to prepare various chiral molecules based on azulenes.

Conflicts of interest

There are no conflicts to declare.

Acknowledgements

This work was supported by the ERATO program from JST (JPMJER1302 to K.I.), the JSPS KAKENHI Grant Numbers (JP16H00907, JP17K19155 and JP18H02019 to H.I.) and the DAIKO Foundation (H.I.). We thank Dr. Yasutomo Segawa, Dr. Hirotoshi Sakamoto, Kenta Kato, Wataru Mastuoka, Michihisa Toya for X-ray diffraction analyses, experimental help and discussions. ITbM is supported by the World Premier International Research Center Initiative (WPI), Japan.

Notes and references

1 For reviews on helicenes, see: (a) Y. Shen and C.-F. Chen, *Helicenes Chemistry: From Synthesis to Applications*, Springer, Berlin, 2017; (b) Y. Shen and C.-F. Chen, *Chem. Rev*., 2012, **112**, 1463; (c) M. Gingras, *Chem. Soc. Rev.,* 2013, **42**, 968; (d) M. Gingras, G. Félix and R. Peresutti, *Chem. Soc. Rev.,* 2013, **42**, 1007; (e) M. Gingras, *Chem. Soc. Rev*., 2013, **42**, 1051; (f) M. Hasan and V. Brovrkoovvko, *Symmetry* 2018, **10**, 10; (g) K. Kato, Y. Segawa and K. Itami, *Synlett,* 2019, **30**, 370.

2 Selected examples: (a) M. Siczek and P. J. Chmielewski, *Angew. Chem., Int. Ed*., 2007, **46**, 7432; (b) M. Yamada, P. Rivera-Fuentes, W. B. Schweizer and F. Diederich, *Angew. Chem., Int. Ed.,* 2010, **49**, 3532; (c) T. Bruhn, G. Pescitelli, S. Jurinovich, A. Schaumlöffel, F. Witterauf, J. Ahrens, M. Bröring and G. Bringmann, *Angew. Chem., Int. Ed.,* 2014, **53**, 14592; (d) W. Yang, G. Longhi, S. Abbate, A. Lucotti, M. Tommasini, C. Villani, V. J. Catalano, A. O. Lykhin, S. A. Varganov and W. A. Chalifoux, *J. Am. Chem. Soc*., 2017, **139**, 13102; (e) Y. Inoue, D. Sakamaki, Y. Tsutsui, M. Gon, Y. Chujo and S. Seki, *J. Am. Chem. Soc*., 2018, **140**, 7152.

3 (a) S. Ito and N. Morita, *Eur. J. Org. Chem*., 2009, 4567; (b) S. Ito, T. Shoji and N. Moritac, *Synlett*, 2011, 2279; (c) H. Xin and X. Gao, *ChemPlusChem,* 2017, **82**, 945.

4 (a) S. A. Pfau and P. A. Plattner, *Helv. Chim. Acta,* 1939, **22**, 202; (b) D. M. Lemal and G. D. Goldman, *J. Chem. Educ*., 1988, **65**, 923.

5 J. Michl and E. W. Thulstrup, *Tetrahedron,* 1976, **32**, 205.

6 (a) F. K. Wang, Y. H. Lai, N. M. Kocherginsky and Y. Y. Kosteski, *Org. Lett*., 2003, **5**, 995; (b) F. K. Wang, Y. H. Lai and M. Y. Han, *Macromolecules,* 2004, **37**, 3222.

7 (a) S. Ito, T. Kubo, N. Morita, T. Ikoma, S. Tero-Kubota and A. Tajiri, *J. Org. Chem*., 2003, **68**, 9753; (b) X. Wang, J. K.-P. Ng, P. Jia, T. Lin, C. M. Cho, J. Xu, X. Lu and C. He, *Macromolecules,* 2009, **42**, 5534.

8 (a) E. Amir, R. J. Amir, L. M. Campos and C. J. Hawker, *J. Am. Chem. Soc*., 2011, **133**, 10046; (b) M. Koch, O. Blacque and K. Venkatesan, *Org. Lett*., 2012, **14**, 1580; (c) M. Murai, E. Amir, R. J. Amir and C. J. Hawker, *Chem. Sci*., 2012, **3**, 2721; (d) K. Tsurui, M. Murai, S.-Y. Ku, C. J. Hawker and M. J. Robb, *Adv. Funct. Mater*., 2014, **24**, 7338; (e) M. Murai, K. Takami, H. Takeshima and K. Takai, *Org. Lett*., 2015, **17**, 1798; (f) K. Ninomiya, Y. Harada, T. Kanetou, Y. Suenaga, T. Murafuji and R. Tsunashima, *New J. Chem.,* 2015, **39**, 9079; (g) E. H. G. Zadeh, S. Tang, A. W. Woodward, T. Liu, M. V. Bondar and K. D. Belfield, *J. Mater. Chem. C*, 2015, **3**, 8495; (h) M. Murai, S. Iba, H. Ota and K. Takai, *Org. Lett.,* 2017*,* **19***,* 5585.

9 (a) H. Salman, Y. Abraham, S. Tal, S. Meltzman, M. Kapon, N. Tessler, S. Speiser and Y. Eichen, *Eur. J. Org. Chem*., 2005, 2207; (b) T. Zieliński, M. Kędziorek and J. Jurczak, *Chem. Eur. J*., 2008, **14**, 838.

10 (a) K. Kurotobi, K. S. Kim, S. B. Noh, D. Kim and A. Osuka, *Angew. Chem., Int. Ed*., 2006, **45**, 3944; (b) A. Muranaka, M. Yonehara and M. Uchiyama, *J. Am. Chem. Soc*., 2010, **132**, 7844.

11 S. Ito, H. Inabe, N. Morita, K. Ohta, T. Kitamura and K. Imafuku, *J. Am. Chem. Soc*., 2003, **125**, 1669.

12 L. Cristian, I. Sasaki, P. G. Lacroix and B. Donnadieu, *Chem. Mater*., 2004, **16**, 3543.

13 (a) Y. Yamaguchi, Y. Maruya, H. Katagiri, K. Nakayama and Y. Ohba, *Org. Lett*., 2012, **14**, 2316; (b) Y. Yamaguchi, K. Ogawa, K. Nakayama, Y. Ohba and H. Katagiri, *J. Am. Chem. Soc.,* 2013, **135**, 19095; (c) J. Yao, Z. Cai, Z. Liu, C. Yu, H. Luo, Y. Yang, S. Yang, G. Zhang and D. Zhang, *Macromolecules,* 2015, **48**, 2039; (d) H. Xin, C. Ge, X. Yang, H. Gao, X. Yang and X. Gao, *Chem. Sci*., 2016, **7**, 6701.

14 (a) M. Ince, J. Bartelmess, D. Kiessling, K. Dirian, M. V. Martínez-Díaz, T. Torres and D. M. Guldi, *Chem. Sci.* 2012, **3**, 1472; (b) E. Puodziukynaite, H.-W. Wang, J. Lawrence, A. J. Wise, T. P. Russell, M. D. Barnes and T. Emrick, *J. Am. Chem. Soc*., 2014, **136**, 11043.

15 H. Nishimura, N. Ishida, A. Shimazaki, A. Wakamiya, A. Saeki, L. T. Scott and Y. Murata, *J. Am. Chem. Soc.,* 2015*,* **137***,* 15656.

16 (a) C. Rosini, L. Franzini, A. Raffaelli and P. Salvadori, *Synthesis,* 1992**,** 503; (b) R. Noyori, *Asymmetric Catalysis in Organic Synthesis*, Wiley, New York, 1994.

17 A.-H. Chen, H.-H. Yen, Y.-C. Kuo and W.-Z. Chen *Synth. Commun*., 2007, **37**, 2975.

18 R. Sigrist and H.-J. Hansen, *Helv. Chim. Acta,* 2014, **97**, 1165.

19 (a) Chaolumen, M. Murata, Y. Sugano, A. Wakamiya and Y. Murata, *Angew. Chem., Int. Ed.,* 2015, **54**, 9308; (b) Chaolumen, M. Murata, A. Wakamiya and Y. Murata, *Angew. Chem., Int. Ed*., **2017**, *129,* 5164; (c) Chaolumen, M. Murata, A. Wakamiya and Y. Murata, *Org. Lett*., **2017**, *19*, 826.

20 J. Wu, Ž. Tomović, V. Enkelmann and K. Müllen, *J. Org. Chem.,* 2004*,* **69***,* 5179.

21 (a) L. Zhai, R. Shukla, S. H. Wadumethrige and R. Rathore, *J. Org. Chem.,* 2010, **75**, 4748; (b) M. Grzybowski, K. Skonieczny, H. Butenschön and D. T. Gryko, *Angew. Chem., Int. Ed.,* 2013, **52**, 9900.

22 K. Uehara, P. Mei, T. Murayama, F. Tani, H. Hayashi, M. Suzuki, N. Aratani and H. Yamada, *Eur. J. Org. Chem.,* 2018*,* 4508.

242x101mm (72 x 72 DPI)